National Conference with International Participation

ENGINEERING MECHANICS 2008

Svratka, Czech Republic, May 12 – 15, 2008

SIMPLIFIED DYNAMIC MODEL OF THE TRANSMISSION

V. Čech[*], J. Jevický[**]

Summary: *Within the framework of the grant project FT–TA3/103 of Ministry of Industry and Trade of the Czech Republic, the prototype of the passive optoelectronic rangefinder (POERF) is developed. A number of subsystems of this rangefinder needs to be solved in this connection. One of these subsystems is the transmission – usually with the same construction for the gearing in the elevation and in the traverse. The accuracy of the measured target coordinates depends both on the accuracy of the measured target range and on the accuracy of the measured target angle coordinates which are taken relatively towards the rangefinder position. The mathematical model of the rangefinder aiming system (special positional servomechanism) is published in Čech (2006). The dynamic model of the transmission is one of its important parts. The corresponding sub model is described in this paper. It makes possible the accuracy analysis of the acquisition process of the target angle coordinates.*

1. Introduction

Mathematical model of the transmission described in this contribution resumes our older model which was published in the paper Čech & Jevický (2005). We have significantly improved the model of stiffness with the inclusion of influence of hysteresis in the gears and the model of losses in the system.

The system is considered to be a system with three degrees of freedom (self-locking transmission) or with two degrees of freedom (other transmissions) respectively. We will suppose nonlinear model with two degree of freedom (2-DOF-NL) in this paper. The application of the model to self-locking transmission will be presented in our next papers.

Models of stiffness have new structures. They allow simulations of impacts of gear backlashes and influences of mechanisms for clearance adjustment, too. The influence of hysteresis losses is included newly.

Traditional models of gear losses make use of *constant* gear efficiency h, e.g. Mudrik (2007). Models fail in situations where the output gearbox torque T_2 is very small or zero ($h \to 0$). These states are very frequent in servomechanisms which allow tracking of slowly moving objects at big distances and so in this case the use of traditional models is impossible. We try to solve the problem by the use of the loss coefficient m_{2B}, which depends on the

[*] Doc. Ing. Vladimír Čech, CSc.: Oprox, a.s., Vnitřní 10, 602 00 Brno; e-mail: cech-vladimir@volny.cz

[**] Doc. RNDr. Jiří Jevický, CSc.: Department of Mathematics and Physics, University of Defence, Kounicova 65, 602 00 Brno; e-mail: jiri.jevicky@unob.cz

relative size of the output load m_2 and on the relative input speed $v = v_1$. The functionalities $m_{2B} = f(m_2, v_1)$, are constructed by the help of data that are provided by transmission-makers and given in catalogues of gearboxes.

We will compare our model (2-DOF-NL) with two traditional *linearized* models of gearboxes. First one has one degree of freedom (1-DOF-L) and second one has two DOF (2-DOF-L). There is supposed that gearbox efficiency is constant ($\eta = const = \eta_C$, Fig. 16). We choose $\eta_C = 0{,}9$ for our analyze.

The efficiency quantity depends on type of the lubricant, its temperature and the wear of the gearbox. There is usually supposed that the lubricant temperature is equal to the ambient temperature and the gearbox wear is insignificant. Catalogue values are given for the ambient temperature equal to approx. 20°C.

The principle of the comparative analysis of the behavior and the characteristics of the gearbox models is presented on Fig. 1. There is the separately exited direct-current motor with constant field, thus the armature control is supposed. The servo-amplifier has a constant voltage gain K_A. The control signal is $E_C = u_C / u_{CR}$ [-] and it is equal to the control signal of the motor $E_Z = u_Z / u_{ZR}$, where u_{ZR} is rated armature voltage ($u_{ZR} = 24$ V) and the rated control voltage is $u_{CR} = u_{ZR} / K_A$. We selected DC motor with rated power approx. 180 W (the rated

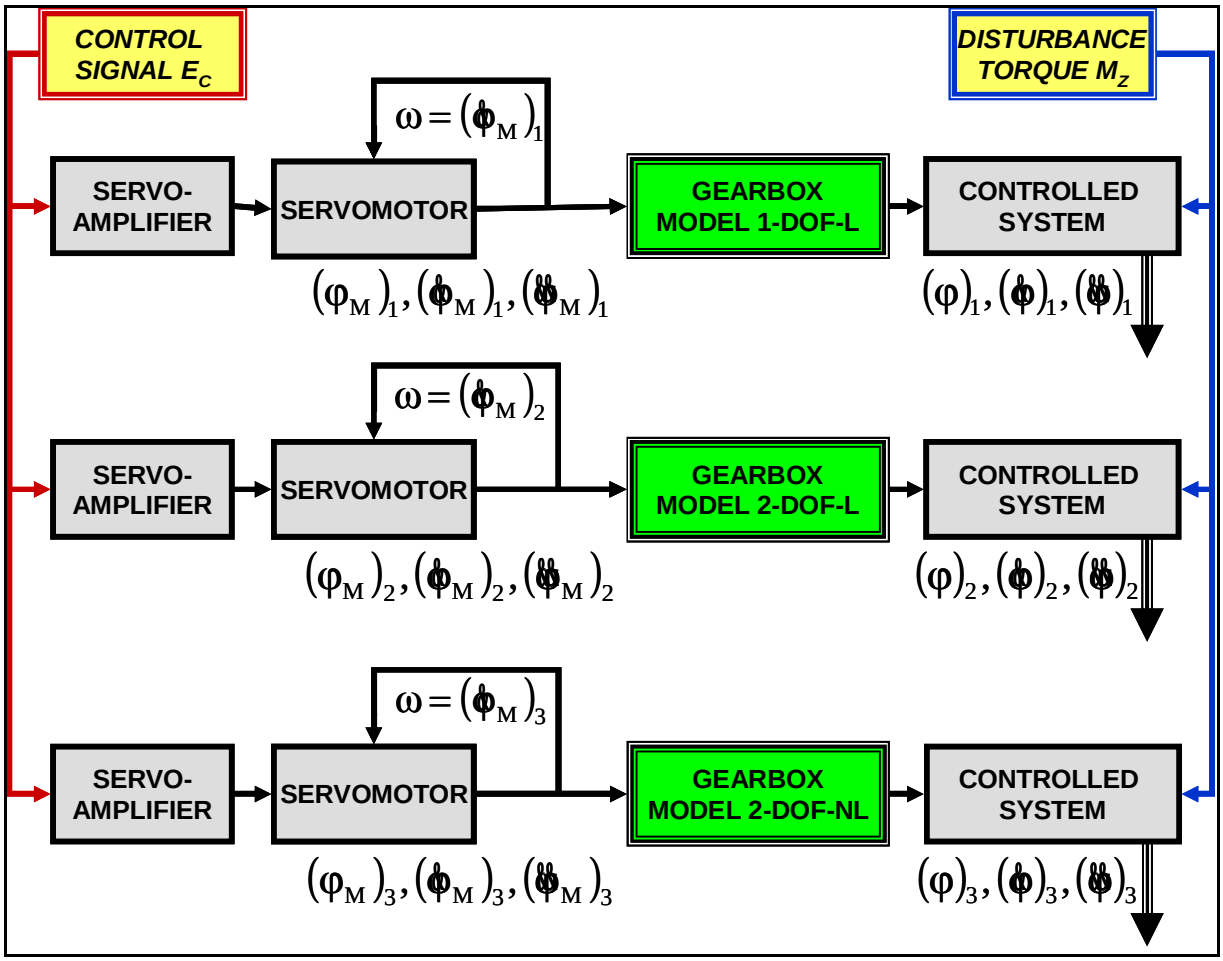

Fig. 1 The principle of the comparative analysis of the behavior and the characteristics of the gearbox models

speed n_{DR} = 3300 rpm or ω_{DR} = 345,6 rad/s and the rated torque M_{DR} = 0,521 Nm) and with the moment of the rotor inertia $J_M = 80 \cdot 10^{-7}$ kgm^2.

The next form of control signal is supposed in this paper

$$E_C = E_{CM} + E_{CA} \cdot sin(w \cdot t + j_{EC}) \quad and \quad w = 2p \cdot f_C , \tag{1}$$

where is selected E_{CM} = 0 and φ_{EC} = 0. We chose two values of the amplitude E_{CA} 1,0275 and 0,025 for the illustration of gearbox models features.

The controlled system is chosen as a very easy mechanical system – the static and dynamic balanced rotational rigid body with its moment of inertia J_Z = 2 kgm^2. The effects of the bearings are represented by the coefficient of viscous friction b_{ZR} ($b_{ZR} = 2\xi_Z \cdot \Omega_Z \cdot J_Z$, ξ_Z = 0,02 – Fig 3.).

The disturbance torque is set equal to zero (M_Z = 0 Nm) in this paper.

The gearbox is represented by the rated input speed n_{1R} = 3630 rpm, the rated output torque T_{2R} = 51,6 Nm, the (kinematics') gear ratio i_C = 90, the moment of inertia (gear input) $J_R = J_{T1} = 67 \cdot 10^{-7}$ kgm^2, the maximal value of the (output) torsional stiffness $k_{2max} = 26{,}5 \cdot 10^3$ Nm/rad (Fig. 7) and the average efficiency of hysteresis process η_H = 0,93 (Fig. 8) in general. The effects of the bearings on the input shaft are represented by the coefficient of viscous friction b_{MR} ($b_{MR} = 2\xi_M \cdot \Omega_M \cdot J_{MR}$, ξ_M = 0,02 – Fig 3.). The relative value of the torsional stiffness $k_{20} = k_{20}/k_{2max}$ for the model 2-DOF-L is chosen by 0,65 (Fig. 3).

The behavior of the DC motor is described by differential equation (armature loop)

$$t_a \cdot \frac{dm_D}{dt} + m_D = k_N \cdot E_Z - (k_N - 1) \cdot \left(\frac{j_M}{w_{DR}} \right), \tag{2}$$

where $m_D = M_D/M_{DR}$ [-] is the relative value of motor driving moment M_D (Fig. 2),
t_a is the electrical (torque) time constant (t_a = 0,1286 ms),
k_N is armature voltage constant (k_N = 3,1169) and
j_M is the angle frequency (speed) of motor rotor and input shaft of the gearbox [rad/s].

We suppose next two equations of motion in general (Fig. 2)

$$\begin{aligned} J_{MR} \cdot \ddot{j}_M + b_{MR} \cdot j_M &= (M_D - T_{10} \cdot sign\, j_M) - T_1 \\ J_Z \cdot \ddot{j} + b_{ZR} \cdot j &= T_2 - M_Z \end{aligned}, \tag{3a,b}$$

where T_{10} is the torque amplitude of the frictional effects of the motor bearings (T_{01} = 0,016 Nm),
T_1 (T_2) is the input (output) torque of the gearbox [Nm] and
j is the angle frequency (speed) of controlled system and output shaft of the gearbox [rad/s].
The „distortion" of the gearbox is defined by next expression (Fig. 3, 6, 7)

$$Dj_2 = \frac{j_M}{i_C} - j , \tag{4}$$

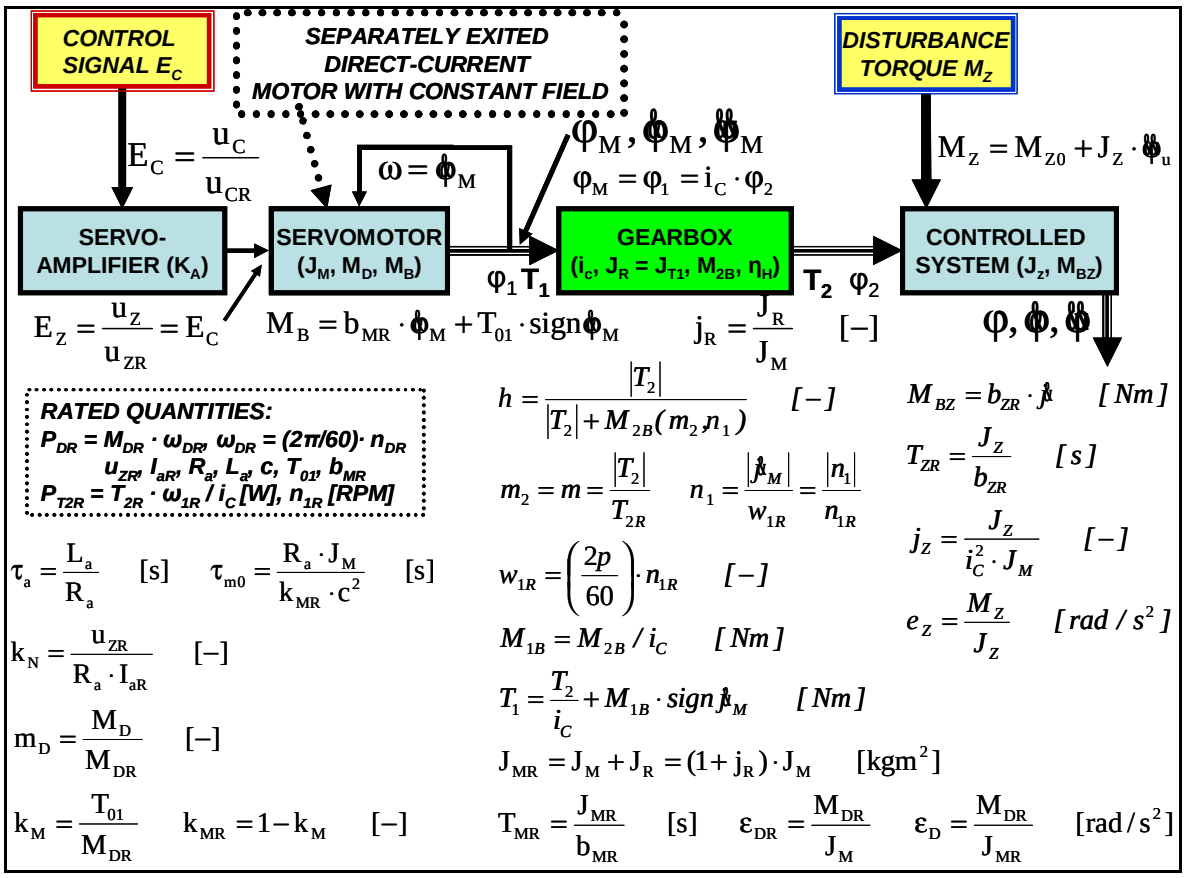

Fig. 2 General definition of the parameters of analyzed systems

2. Traditional models of the gearbox

Firstly, we start with analyze of the 2-DOF-L model (Fig. 2, 3). There are given two postulate

$$T_2 = k_{20} \cdot Dj_2 \qquad k_{20} = const \qquad and \qquad T_1 = \frac{T_2}{i_C \cdot h_C}, \tag{5a,b}$$

Using this postulate and equations (3a,b) we obtain after rearrangement next two equations of motion

$$\begin{aligned} &\ddot{\phi}_M + 2 \cdot x_M \cdot W_M \cdot \dot{\phi}_M + W_M^2 \cdot (j_M - i_C \cdot j) = e_D \cdot (m_D - k_M \cdot \text{sign}\dot{\phi}_M) \\ &\ddot{\phi} + 2 \cdot x_Z \cdot W_Z \cdot \dot{\phi} + W_Z^2 \cdot \left(j - \frac{j_M}{i_C}\right) = -e_{DRZ} \cdot m_Z \end{aligned}, \tag{6a,b}$$

Mechanical system has resonant (peak) frequency. Its upper estimation is given by undamped natural frequency f_{T0} (Ω_{T0}) which is equal to 65,5 Hz. This quantity and the quantity of time constant τ_a are determined the upper limit of the numerical integration step.

The 1-DOF-L model is based on postulate of the absolute rigidity of parts of the gearbox, thus

$$Dj_2 \equiv 0 \qquad or \qquad j = \frac{j_M}{i_C}. \tag{7}$$

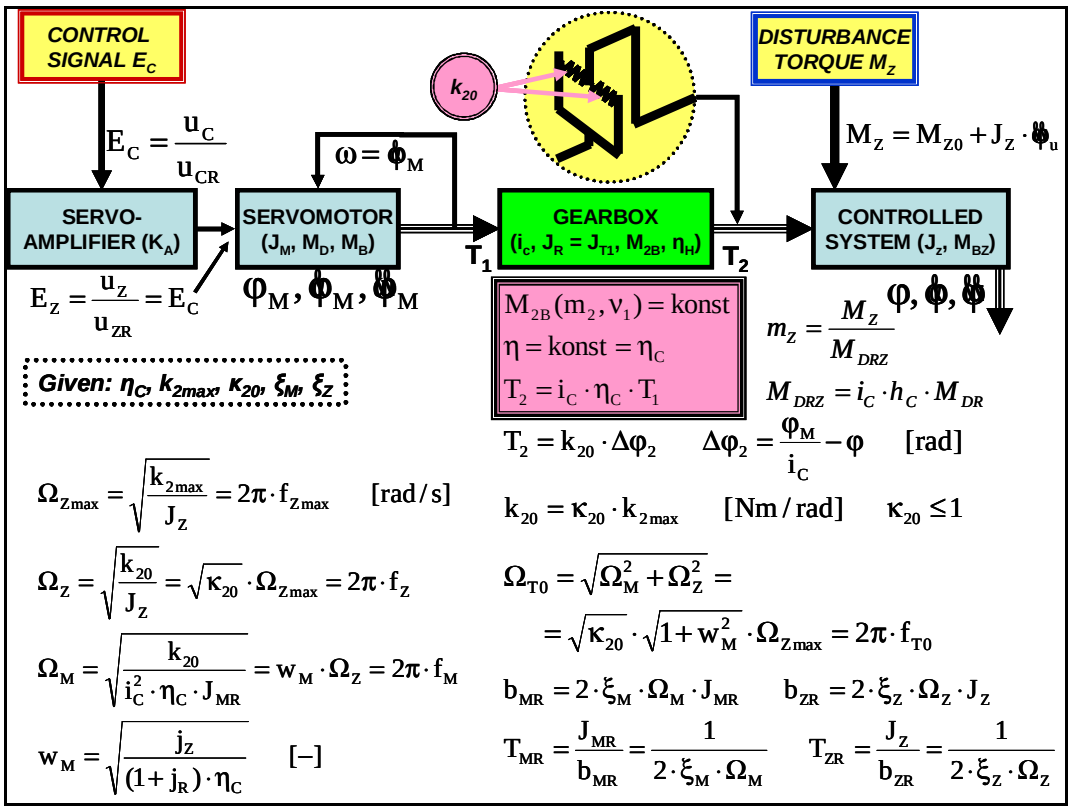

Fig. 3 Definitions for parameters of the 2-DOF-L model

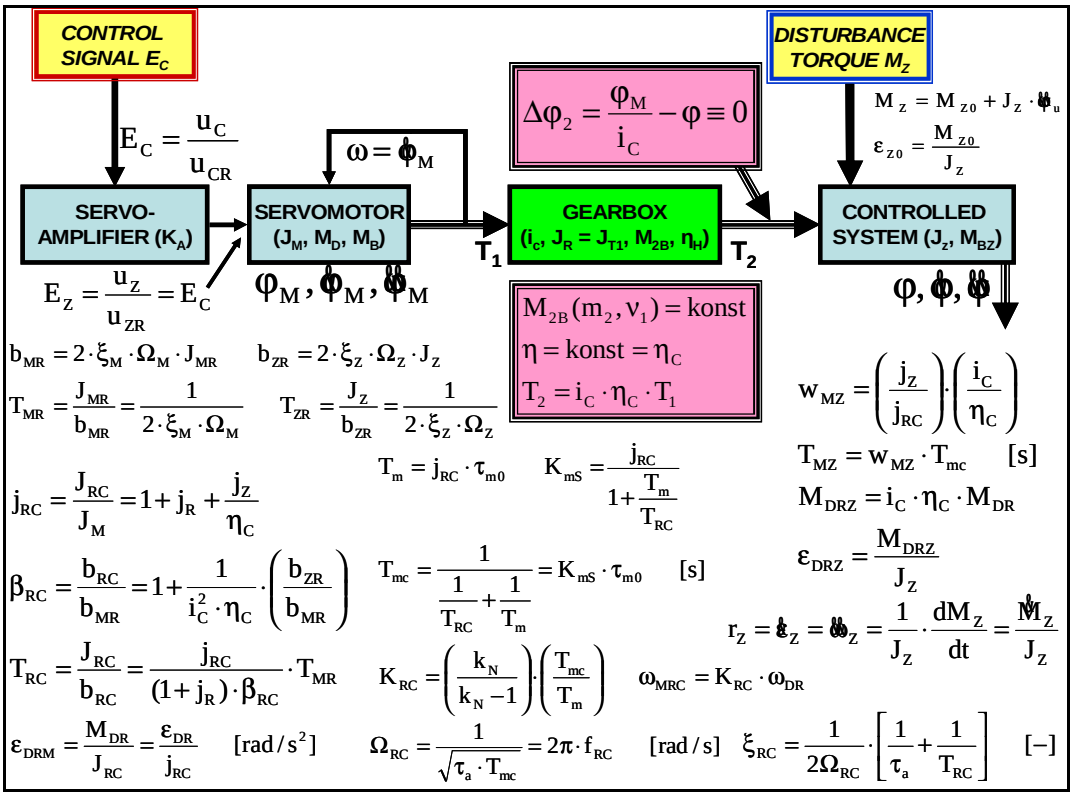

Fig. 4 Definitions for parameters of the 1-DOF-L model

Using this postulate and equations (3a,b) we obtain after rearrangement next equation of motion (Fig. 4, j_{RC} = 36,1, β_{RC} = 5,32, T_{RC} = 233,4 ms)

$$\ddot{\varphi}_M + \frac{1}{T_{RC}} \cdot \dot{\varphi}_M = e_{DRM} \cdot \left[(m_D - k_M \cdot sign\,\dot{\varphi}_M) - m_Z \right], \tag{8}$$

We can combine equations (2) and (8) in next step to get basic equation of the 1-DOF-L model ($m_D - k_M \cdot sign\,\dot{\varphi}_M \cong m_D$)

$$\dddot{\varphi}_M + 2 \cdot x_{RC} \cdot W_{RC} \cdot \ddot{\varphi}_M + W_{RC}^2 \cdot \dot{\varphi}_M = W_{RC}^2 \cdot \left[w_{MRC} \cdot E_Z - T_{MZ} \cdot \left(e_Z + t_a \cdot \ddot{e}_Z \right) \right], \tag{9}$$

where $\Omega_{RC} = 2p \cdot f_{RC}$ is the characteristic angular frequency (f_{RC} = 56,6 Hz),
ξ_{RC} is the damping ratio (ξ_{RC} = 10,9),
ω_{MRC} is the steady–state rated angular frequency of the system (ω_{MRC} = 374,8 rad/s,E_{CA} = 1),
T_{MZ} is the time constant (T_{MZ} = 5,17 s),
t_{m0} is the electromechanical (speed) time constant of the DC motor (t_{m0} = 2,31 ms) and
T_{mc} is the time constant of the system (T_{mc} = 61,48 ms).

The frequency response of the system, which is described by equation (8), is characterized by the normalized magnitude $g(\omega)$ and the phase $\varphi(\omega)$

$$g(w) = \left(\frac{1}{w_{MRC}} \right) \cdot \frac{F(\dot{\varphi}_M)}{F(E_Z)} = \left(\frac{i_C}{w_{MRC}} \right) \cdot \frac{F(\dot{\varphi})}{F(E_Z)} = \frac{1}{\sqrt{\left[\left(1 - l^2\right)^2 + 4 \cdot x_{RC}^2 \cdot l^2 \right]}} \qquad l = \frac{w}{W_{RC}} = \frac{f_C}{f_{RC}}, \tag{10}$$

$$j(w) = arctg\left(-\frac{2 \cdot x_{RC} \cdot l}{1 - l^2} \right). \tag{11}$$

The cutoff frequency of this system is $f_{-3dB} \approx$ 2,6 Hz ($\lambda_{-3dB} \approx$ 0,0458) (Fig. 17, 18).

3. Advanced model of the gearbox

Our advanced 2-DOF-NL model is described by adapted equations of motion (3a,b)

$$\ddot{\varphi}_M + \frac{1}{T_{MR}} \cdot \dot{\varphi}_M = e_D \cdot \left[(m_D - k_M \cdot sign\,\dot{\varphi}_M) - t_1 \right], \quad T_1 = \frac{1}{i_C} \cdot \left[T_2 + M_{2B} \cdot sign\,\dot{\varphi}_M \right]$$
$$\ddot{\varphi} + \frac{1}{T_{ZR}} \cdot \dot{\varphi} = e_{DRZ} \cdot \left[t_2 - m_Z \right], \quad t_1 = \frac{T_1}{M_{DR}}, \quad t_2 = \frac{T_2}{M_{DRZ}} \tag{12a,b}$$

and by expressions for torques T_2 and M_{2B}. There are time constants T_{MR} and T_{ZR} (T_{MR} = 62,36 ms, T_{ZR} = 269,4 ms) in equations (12a,b) (Fig. 2, 3, 4).

The torque M_{2B} is determined by loss coefficient function $m_{2B}(m_2, v_1)$ ($M_{2B} = m_{2B} \cdot T_{2R}$). The loss coefficient function $m_{2B}(m_2, v_1)$ is set up by catalogue data of the specific gearbox (Fig. 5) as a two dimensional table. The data are relevant only for the specific type and size of gearboxes.

The principle of the measurement of gearbox characteristics is shown in Fig. 6. The data of the table (Fig. 5), which describe the loss coefficient $m_{2B}(m_2, v_1)$ function, are taken from four sources (Fig. 5 – areas numerate from 1 to 4). The data from areas 1, 2 and 4 are measured by steady-state conditions (ω_1, ω_2, T_1, T_2 = const).

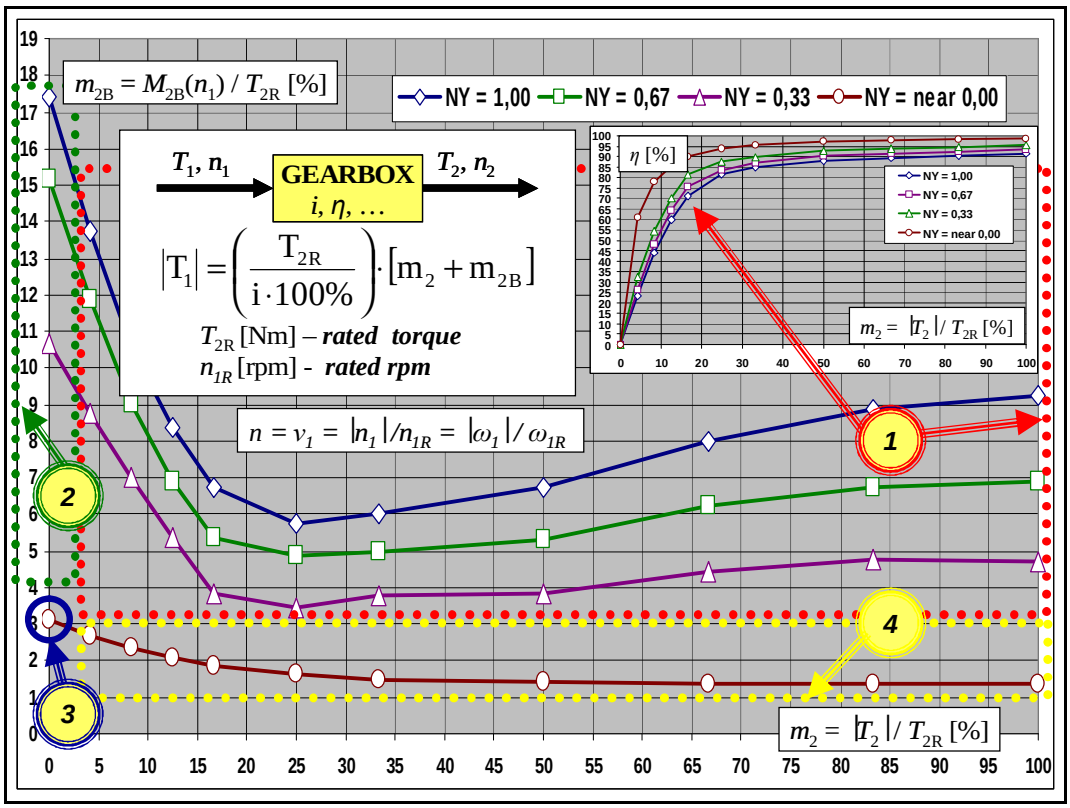

Fig. 5 The plot of the gearbox loss coefficient $m_{2B}(m_2, v_1)$ function – example

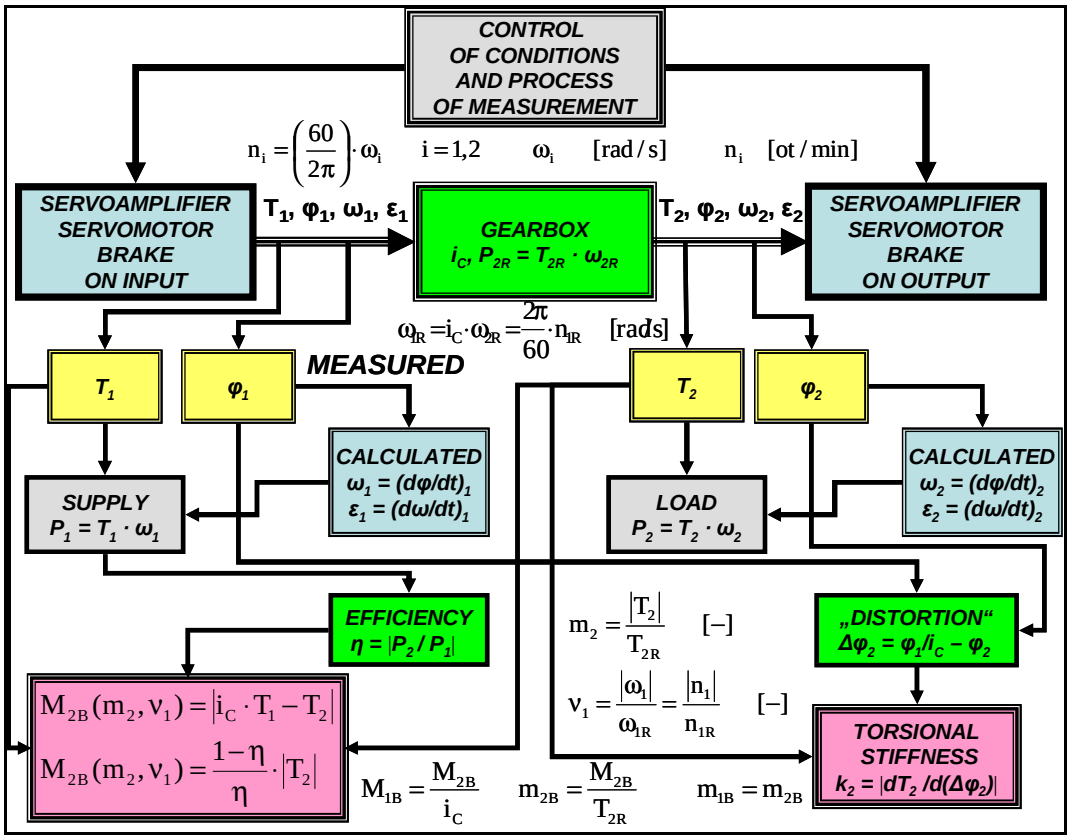

Fig. 6 The principle of the measurement of gearbox characteristics

The data of the first area create the largest part of table or the gearbox loss coefficient $m_{2B}(m_2, v_1)$ function. They are calculate from function of *gearbox efficiency* $\eta(n_1, m_2)$ (Fig. 4, 5).

The data of the second area are adopted from "*no load running torque*" $T_1(v_1 > 0, m_2 = 0)$.

The data of the fourth area aren't presented in catalogues $T_1(v_1 \to 0, m_2 > 0)$ and it is a requisite to estimate these using the general knowledge of gearbox behavior.

Only one value $m_{2B}(v_1 = 0, m_2 = 0)$ lies in third area, which is a little biggest as the value $m_{2Bstart} = i_C \cdot T_1(t_0)/T_{2R}$, where $T_1(t_0)$ is the catalogue value "starting torque" $T_{1start}(v_1(t < t_0) = 0$ *and* $v_1(t \geq t_0) > 0, m_2 = 0) = T_1(t_0)$. The starting torque represents the effect of frictional forces in the gearbox at the moment t_0 when its input shaft under the act of the motor (on input, Fig. 6) starts to run.

The principle of the measurement of the gearbox "torsional stiffness" is shown in Fig. 7. The curve of the torsional stiffness $k_2(D\varphi_2)$ is approximated by usually three catalogue values k_{2i}, $i = 1, 2, 3$ plus two catalogue values $D\varphi_{2i}$, $i = 1, 2$ ($D\varphi_{21}$ = 0,6 mrad, $\psi_{22} = 5$, $\kappa_{21} = 0{,}1$, $\kappa_{22} = 0{,}8$, $\kappa_{23} = 1{,}0$). The basic value of the torque T_2 is defined by formula

$$T_{2P} = |T_{2P}| \cdot sign\,\varphi_M\,, \tag{13}$$

where (Fig. 7)

$$|T_{2P}| \cong \begin{bmatrix} k_{21} \cdot |D\varphi_2| & |D\varphi_2| \le D\varphi_{21} \\ T_{2P1} + k_{22} \cdot (|D\varphi_2| - D\varphi_{21}) & |D\varphi_2| \in \langle D\varphi_{21}, D\varphi_{22} \rangle \\ T_{2P2} + k_{23} \cdot (|D\varphi_2| - D\varphi_{22}) & |D\varphi_2| \ge D\varphi_{22} \end{bmatrix}. \tag{14}$$

The final expression of torque T_2 is complying with the hysteresis loop (Fig. 8)

$$T_2 = T_{2P} + DT_{2H}(t)\,, \tag{15}$$

where torque $DT_{2H}(t)$ represent the effect of the "gearbox hysteresis"

$$\begin{aligned} DT_{2H}(t) &= DT_{Hi} \cdot sign D\varphi_2(t_{0i}) \quad for \quad t \in \langle t_i, t_{i+1} \rangle \\ DT_{Hi} &= \frac{1}{2} \cdot (1 - h_H) \cdot |T_{2P}(t_{0i})| \quad i = 0,1,2,... \end{aligned}\,, \tag{16a,b}$$

t_{0i}, $i = 0, 1, 2, \ldots$ is the set of time points in which is fulfilled the condition $D\varphi_2(t) = 0$, η_H is the average efficiency of hysteresis process (η_H = 0,93).

4. Simulation experiments

There are two parts of the show of the simulations experiments outputs. The first section (Fig. 9 to 16) demonstrated the behavior of our advanced model 2-DOF-NL. The second part (Fig. 17, 18) gives short comparison of the frequency response functions generated by the models 1-DOF_L and 2-DOF-NL.

There are used next parameters of control signal $E_C(t)$, which are employed in the first section - frequency f_C = 1 Hz, amplitude E_{CA} = 1,0275 and 0,025. Their plots are shown on Fig. 9 and 10 together with the corresponding relative values $m_D(t)$ of the motor driving torque M_D.

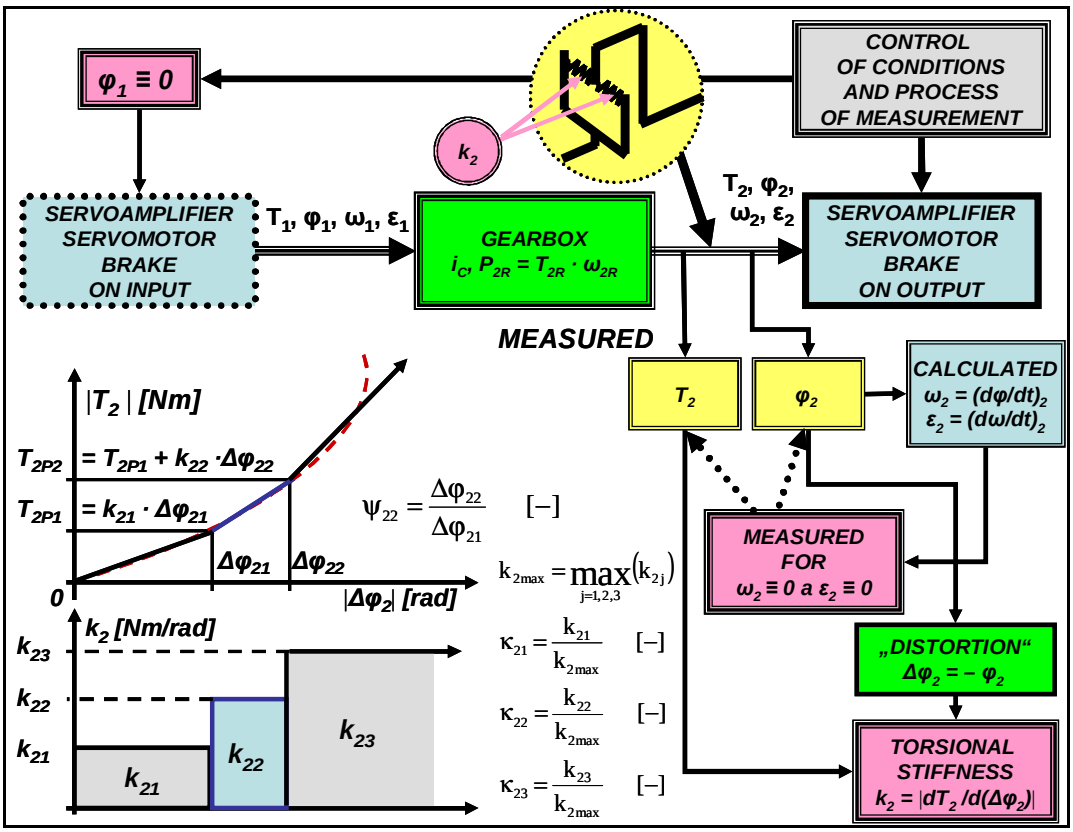

Fig. 7 The principle of the measurement of the gearbox “torsional stiffness”

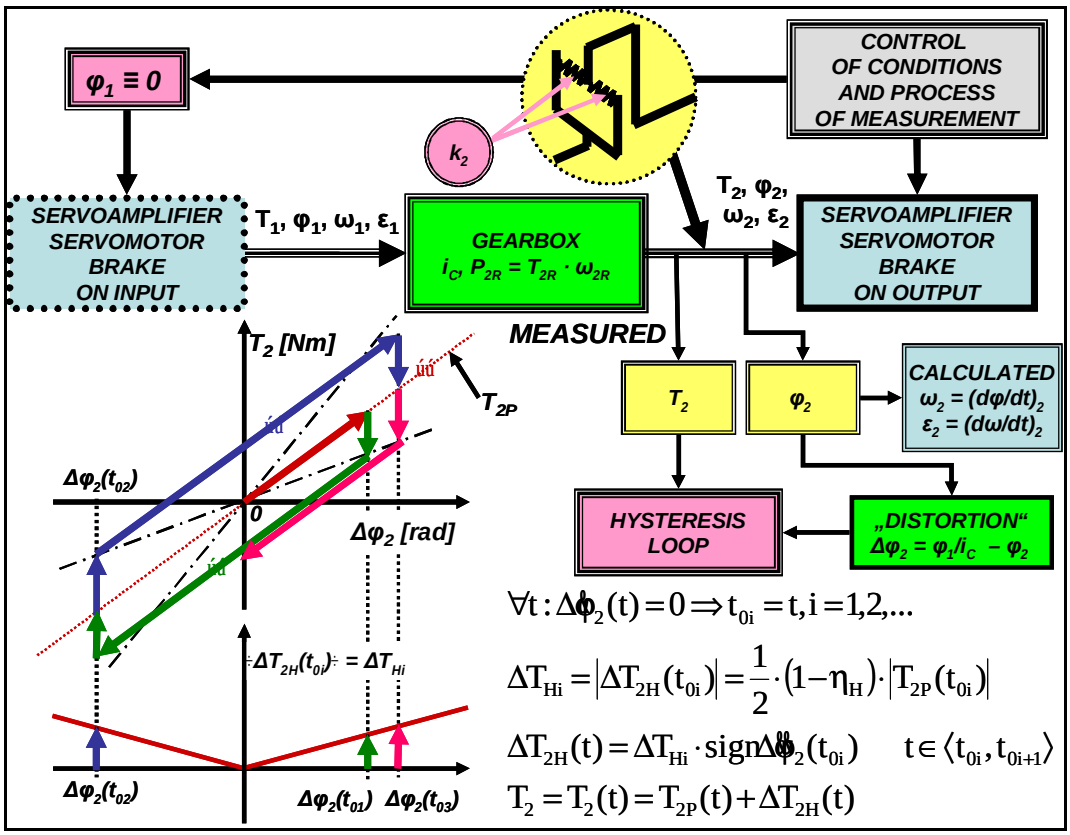

Fig. 8 The principle of the measurement of the gearbox “hysteresis loop”

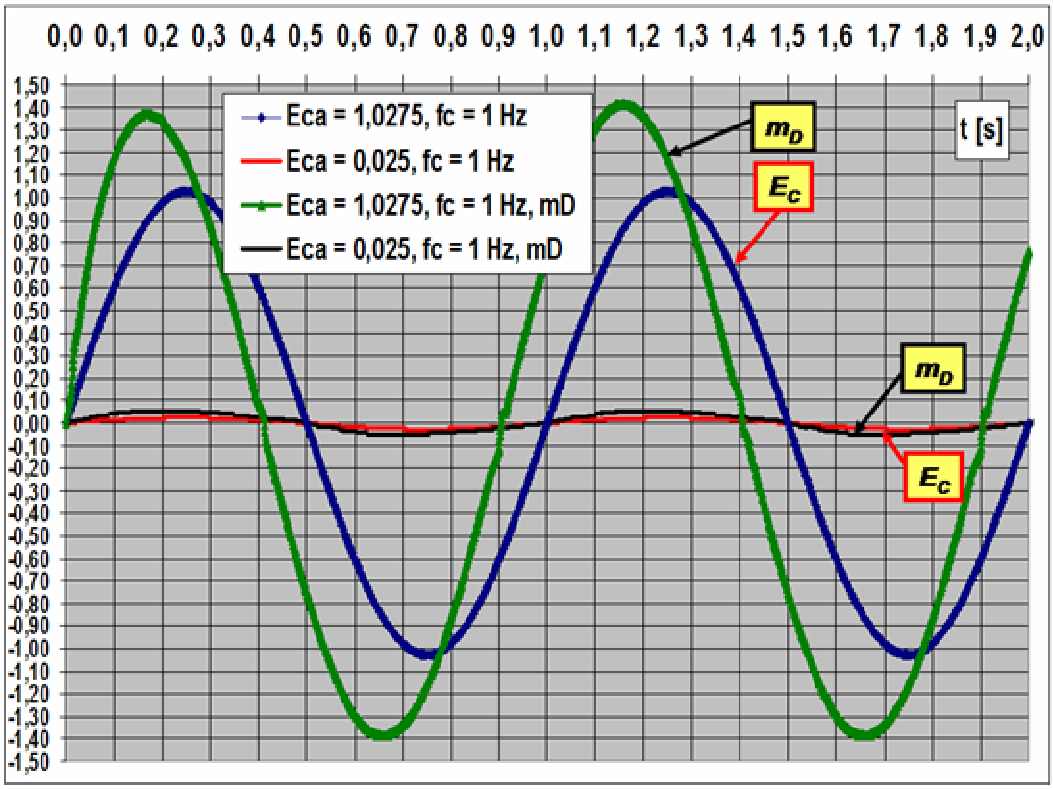

Fig. 9 The control signals $E_C(t)$ and relative motor driving torques $m_D(t)$ plots

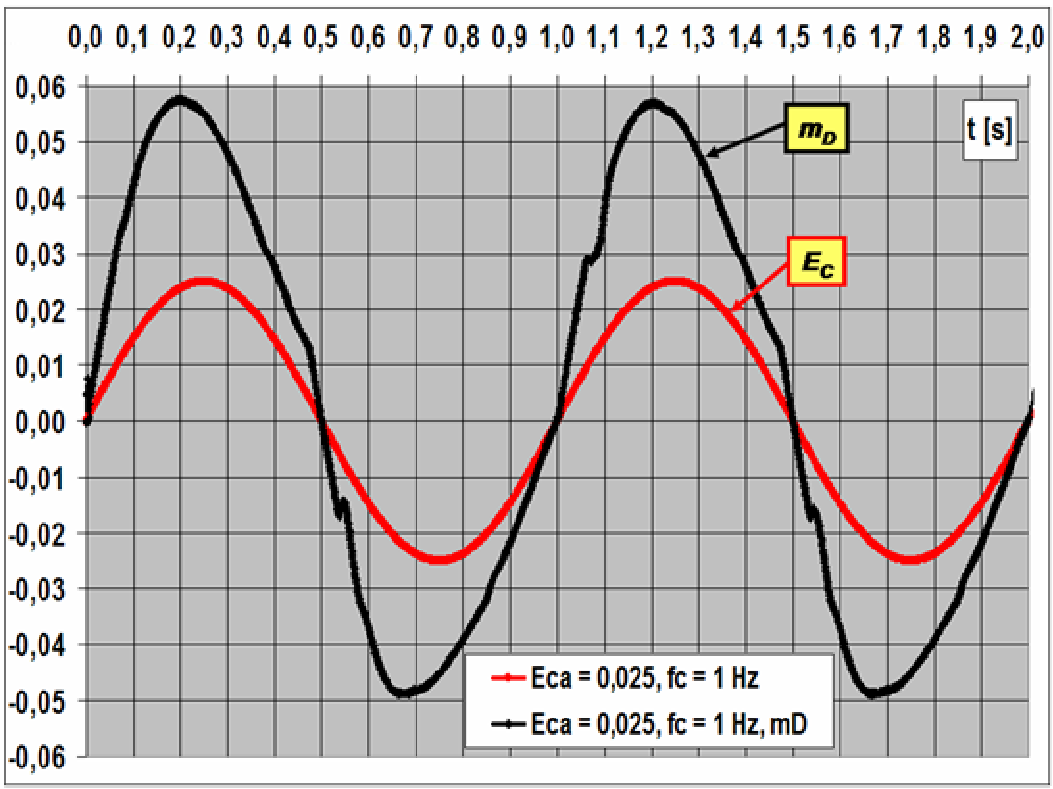

Fig. 10 Plots details of Fig. 9

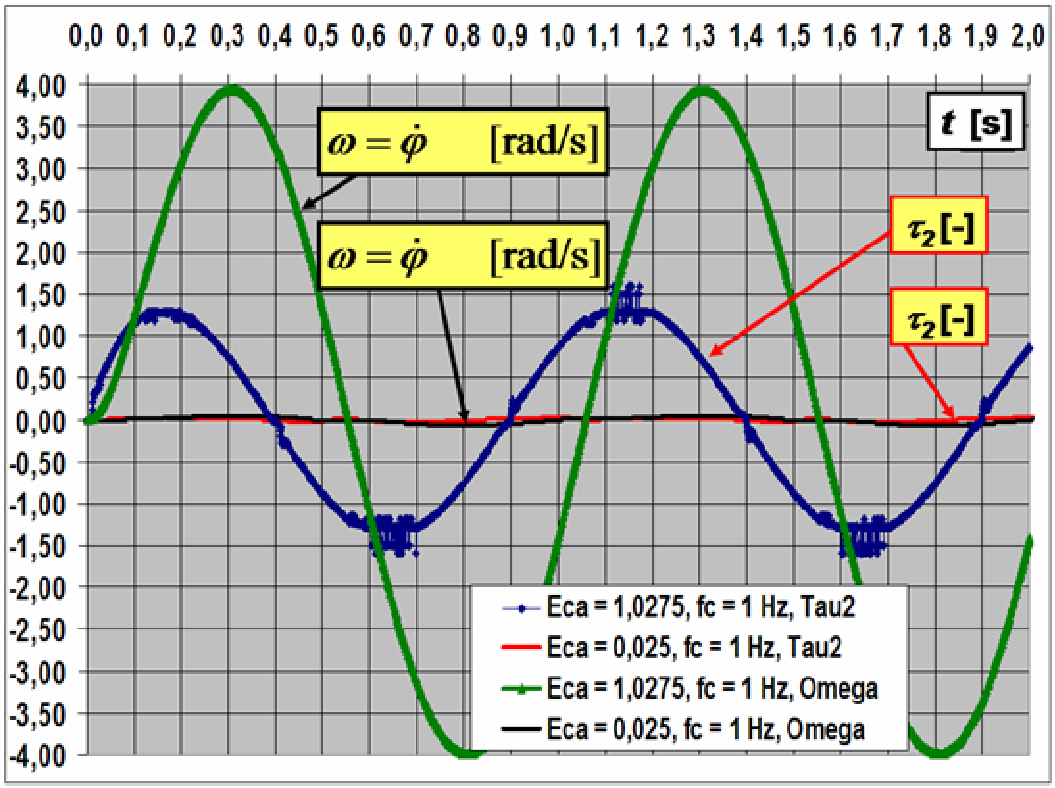

Fig. 11 Plots of the instantaneous angular frequency ω of the controlled system and plots of the instantaneous relative value t_2 of the torque T_2

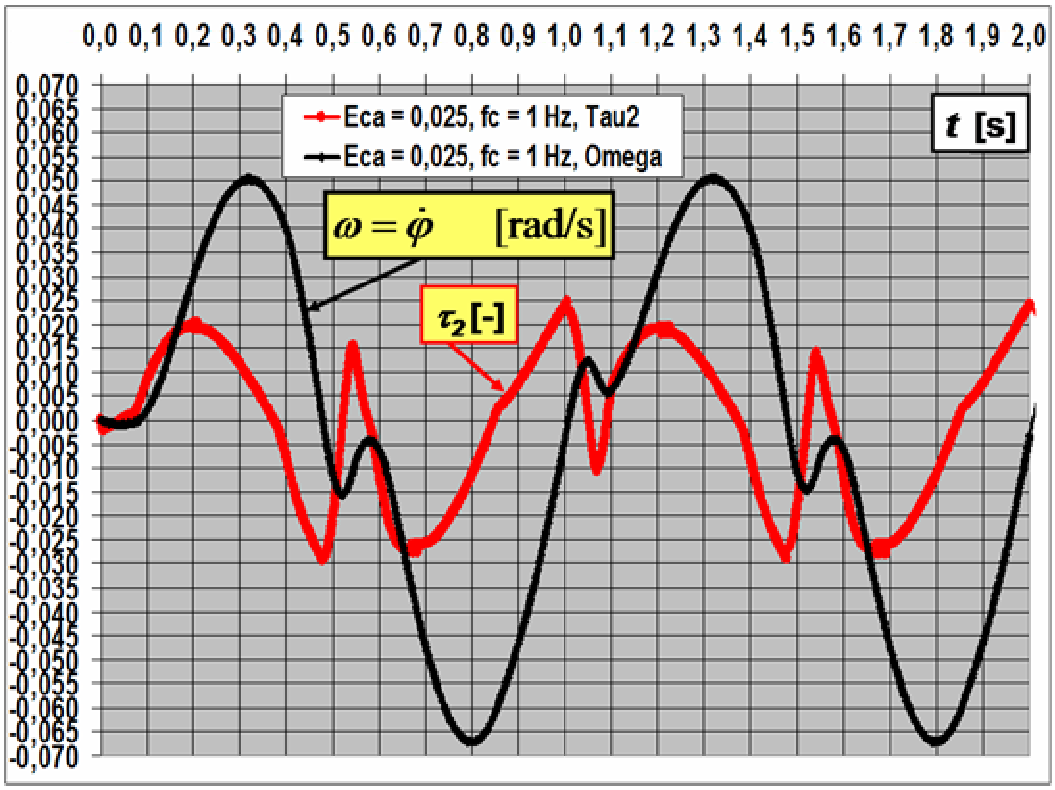

Fig. 12 Plots details of Fig. 11

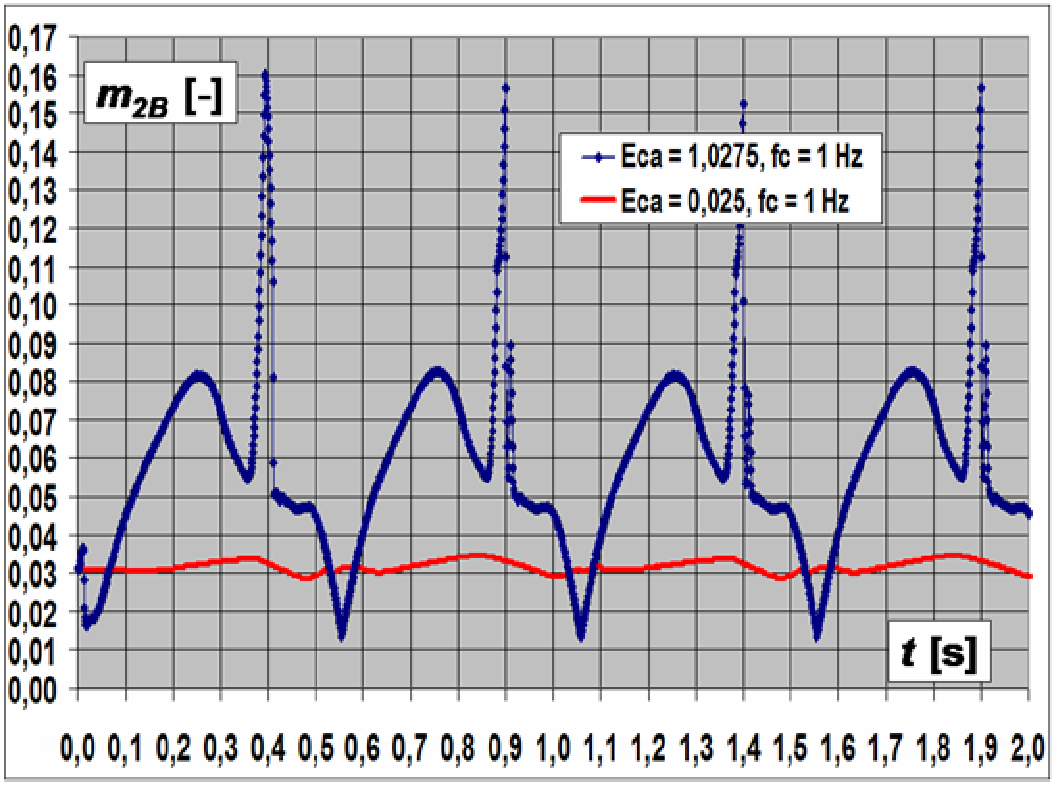

Fig. 13 Plots of the instantaneous values of the loss coefficient $m_{2B}(v_1, m_2)$

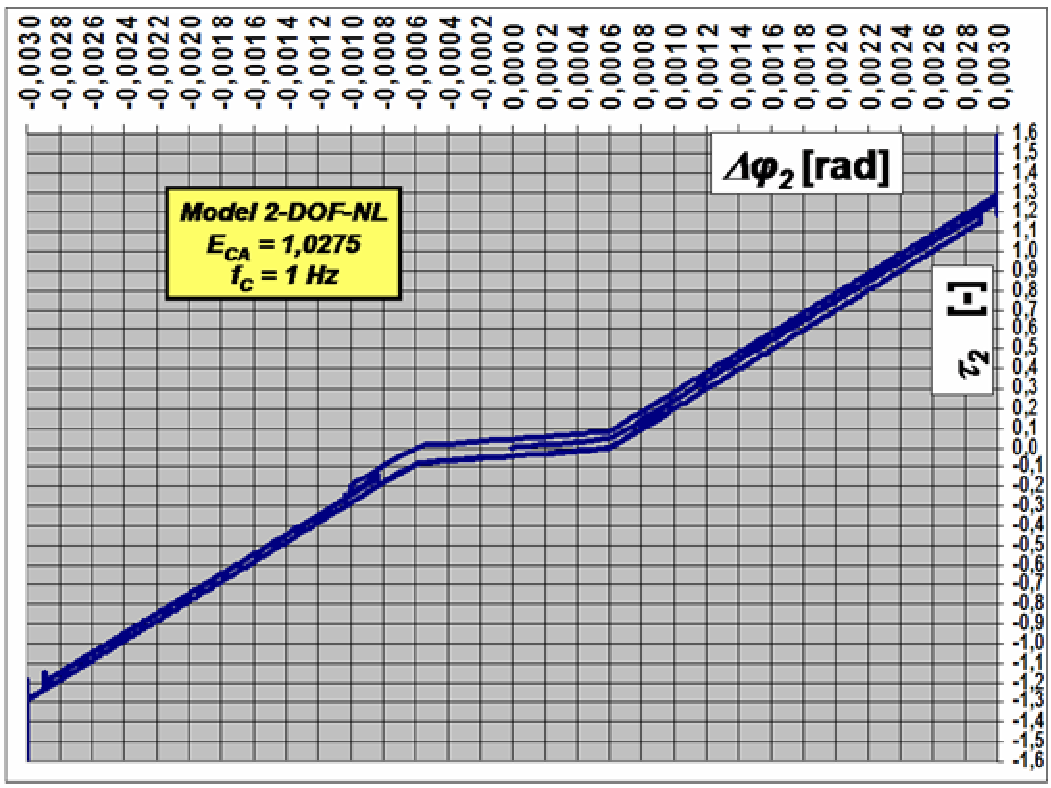

Fig. 14 Plots of the normalized hysteresis loop

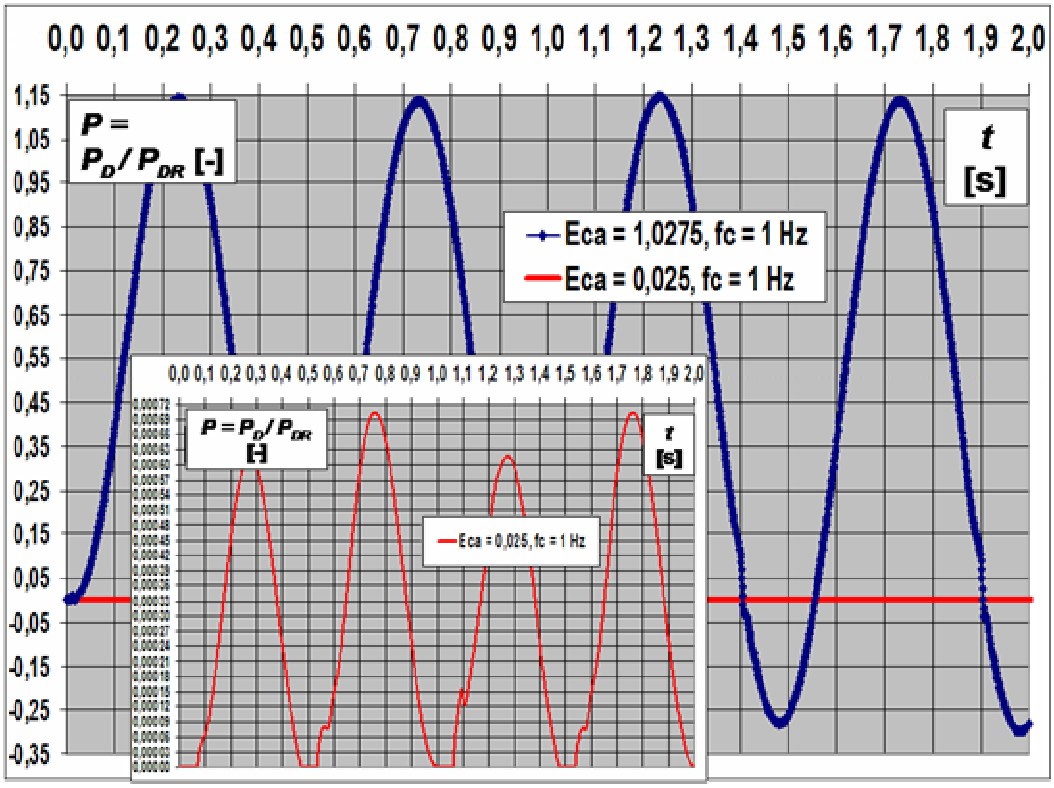

Fig. 15 Plots of the instantaneous values of the normalized motor power *p(t)*

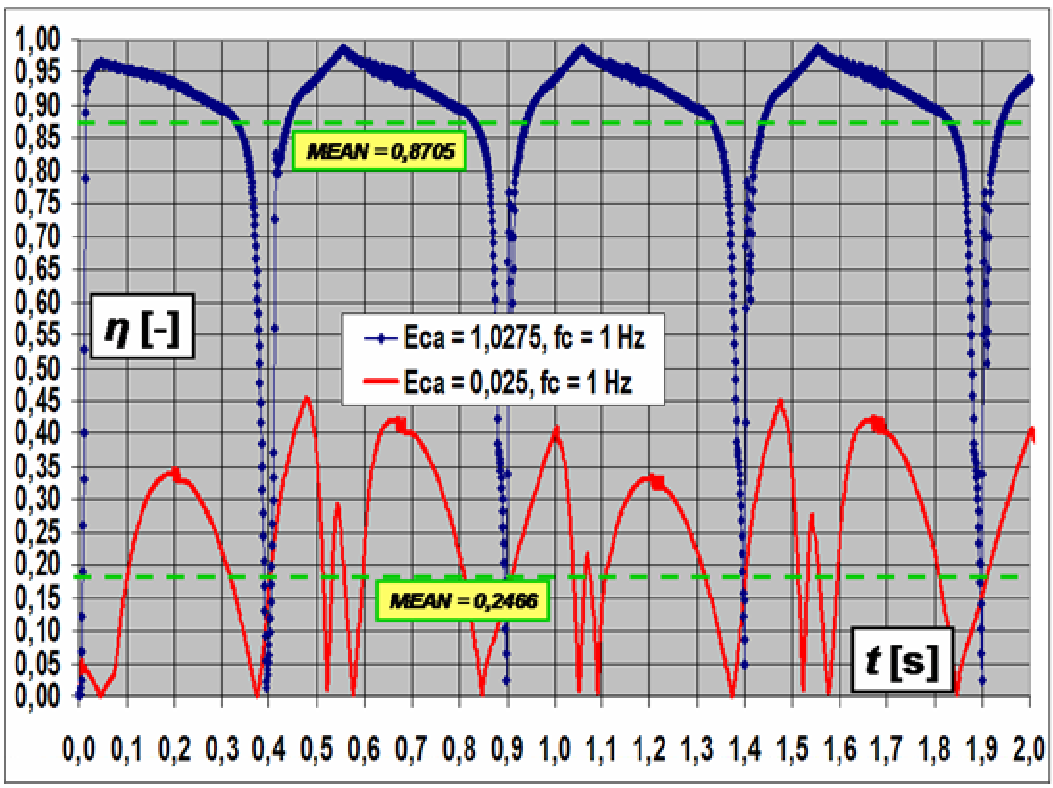

Fig. 16 Plots of the instantaneous gearbox efficiency *η(t)*

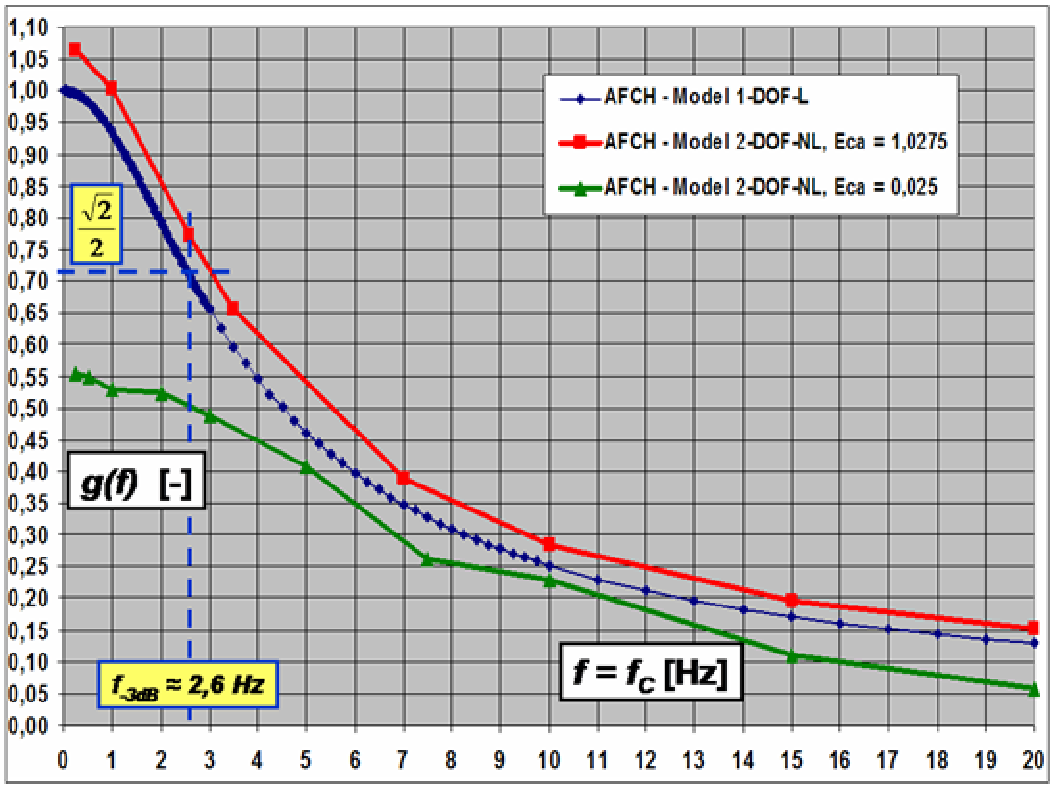

Fig. 17 Frequency response – normalized magnitude plots *g(f)*

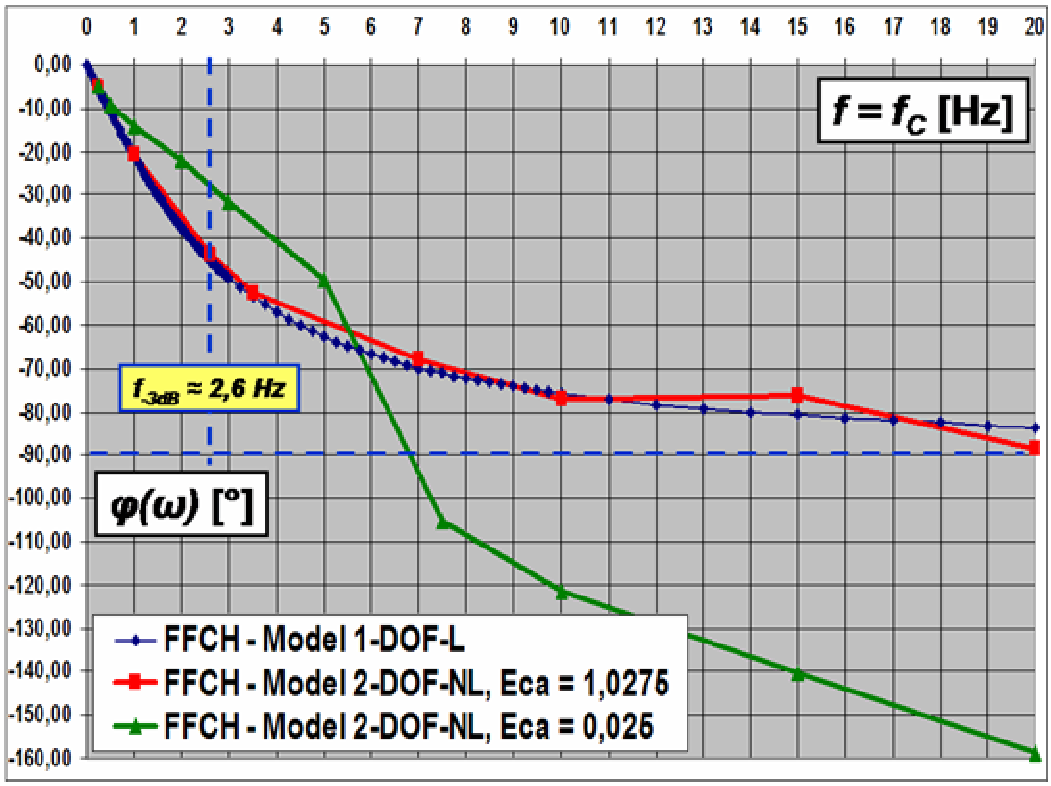

Fig. 18 Frequency response – phase plots $\varphi(\omega) = \varphi(f)$

Plots of the instantaneous angular frequency ω of the controlled system and plots of the instantaneous relative value τ_2 of the torque T_2 (Fig. 11, 12) give information about the output of the gearbox. We can examine that the outputs are strong nonlinear distorted for $E_{CA} = 0{,}025$, due to we had to apply the harmonic linearization method to get the equivalent frequency response (Fig. 17, 18).

Plots (Fig. 13) of the instantaneous values of the loss coefficient $m_{2B}(v_1(t), m_2(t))$ offer the possibility to explain the changes in course of the instantaneous gearbox efficiency $\eta(t)$ (Fig. 16).

The shape of the gearbox hysteresis loop is evident from plot on Fig. 14.

Plots (Fig. 15) of the instantaneous values of the normalized motor power $p(t)$ give information about the output power of the motor.

The most important is the instantaneous gearbox efficiency $\eta(t)$ plot (Fig. 16) for understanding, why the traditional models 1-DOF-L and 2-DOF-L malfunctioning in many situations. The basic presumption for the successful application this models in praxis is the a priori knowledge of the average (mean) value of gearbox efficiency η_C. As is obvious from plots, the value η_C depends on the amplitude E_{CA} of control signal and in general on the time-shape of the control signal. When is changed the level of the control signal, then changed the value η_C, too. It induces, that the suitable controller has to be adaptive. Without using our advanced 2-DOF-NL model is very difficult to create it.

The changes of the frequency response (Fig. 17, 18) depending on the E_{CA} greatness are the consequence of η_C changes.

5. Conclusions

We propose that we will analyze the interaction between the gearbox and synchronous AC motor to prepare conditions for the design of the adaptive controller. We will make use of experiments with the direction channel of the POERF. Our final goal is to take part on building of the full operational prototype of the direction channel of the POERF.

We will continue to work on the matching of our advanced model for self-locked gearboxes.

Acknowledgement

This work has originated under the support of financial means from the industrial research project of the Ministry of Industry and Trade of the Czech Republic – project code FT – TA3/103: "Research of high-end technologies and methods for recognition of moving objects, determination of parameters of objects' motion and for systems of automatic tracking of moving objects".

Reference

Balátě, J. (2004) Automatic control (2nd edition). Praha, BEN , 664 pages

Bolek, A. & Kochman, J. et al. (1990) Machine elements. 2nd volume (Technický průvodce 6). Praha, SNTL, 712 pages

Čech, V. & Jevický, J. (2005) Simplified dynamic model of the self-locking transmission. (In Czech.) In Proceedings of Colloquium Dynamics of Machines 2005, Praha, 8.- 9.2.2005, pp. 15-22, ISBN 80-85918-79-X.

Čech, V. (2006) Systemic study to the evaluation of system solution and the accuracy of measurement of targets range by passive optoelectronic rangefinder. (In Czech.) The part of the industrial research project of MIT CR FT – TA3/103. Brno. 281 pages.

Juliš, K. – Brepta, R. et al. (1987) Mechanics – Dynamics – Technický průvodce 66, Praha, SNTL, 688 pages

Mudrik, J. (2007) Engine drive with locking mechanisms. In Book of Extended Abstracts of Engineering Mechanics 2007 and Proceedings on CD-ROM, Svratka, 14.- 17.5.2007, pp. 189-190, ISBN 978-80-87012-06-2.

Catalogues of Twinspin Bearing Reducers (Cycloidal reducers), Kimex, s.r.o., Košice. www.twinspin.sk

Catalogues of Harmonic Drive LLC. Harmonic drive gearing. Precision Gearing and motion. Control. Miniature gearheads. www.harmonicdrive.net/products/gearheads/